Theory of the quasioptical electron cyclotron maser

P. Sprangle, J. L. Vomvoridis,* and W. M. Manheimer
Plasma Physics Division, U.S. Naval Research Laboratory, Washington, D.C. 20375
(Received 9 October 1980)

In this work a promising new electron cyclotron maser oscillator is proposed and analyzed. The configuration utilizes an open resonator cavity containing a gyrating electron beam which translates along an external magnetic field. The magnetic field is directed perpendicular to the axis of symmetry of the open resonator. Because the wave-particle interaction volume is extremely large, the total input electron beam power can be high and the power density low. This configuration has a number of potentially very attractive features. Among them are (i) high operating radiaion power levels (>MWs); (ii) high efficiency operation (>45%); (iii) naturally suited to short wavelength operation (λ <2 mm); (iv) operates efficiently at low electron beam voltage (10–100 keV); (v) natural transverse mode selectivity; (vi) moderate insensitivity to beam temperature effects. The nonlinear interaction between the electrons and resonator field have been analyzed and an expression for the steady-state efficiency obtained. The expression for efficiency has a rather simple analytic form when the amplitude of the resonator fields are small, i.e., small-signal regime. In this case, the efficiency is an essentially odd, nonoscillating function of the frequency mismatch (difference between resonator frequency and relativistic cyclotron frequency). For a uniform external magnetic field, total efficiencies in excess of 30% can be realized. We have considered enhancing the efficiencies by spatially contouring the magnetic field. Appropriately contouring the magnetic field across the resonator by ~5% increases the efficiency from ~35 to ~45%.

I. INTRODUCTION

At the present time, two classical radiation mechanisms, i.e., the free electron laser[1-9] (FEL) and electron cyclotron maser[10-19] (ECM), are under extensive study because of the great potential they show as new classes of coherent radiation sources. Experimental results on the FEL (Refs. 20 and 21) and ECM (Refs. 22–25) have been very encouraging.

In free electron lasers the active medium is a beam of relativistic electrons. Such sources have the potential for generating coherent radiation ranging from the millimeter to the optical regime and beyond. They are frequency tunable and in principle extremely efficient generators of intense radiation.

The electron cyclotron maser in its present form has reached a far more mature stage of development than the FEL. In the millimeter regime, electron cyclotron masers have generated power levels substantially higher and more efficiently than the more conventional radiation sources. Experimental efficiencies are impressive, e.g., 22% efficiency at $\lambda = 2$ mm with a CW output power of 22 kW.[23]

In this paper we propose and analyze a new electron-cyclotron-maser oscillator configuration, which utilizes an open resonator cavity. Our quasioptical cyclotron maser has a unique potential for becoming a new type of coherent radiation source. In principle, the device is capable of generating coherent radiation in the millimeter to submillimeter regime, at power levels in excess of megawatts, with efficiences exceeding 50%. The basic structure consists of an open resonator containing a beam of electrons gyrating about, as well as streaming parallel to, an applied magnetic field. The magnetic field is directed transverse to the axis of the open resonator, which consists of two or more appropriately curved mirrors. Moderately low electron beam energies can be used, i.e., 10–100 keV, even though the wave-particle interaction mechanism is due to relativistic effects. This configuration has a number of distinct advantages over the more conventional radiation sources. Some of these advantages are the following: (i) extremely high operating power levels, (ii) high operating frequency, (iii) high efficiency and, (iv) natural transverse mode selection. Since we utilize an open resonator, and, thus, have a large interaction volume, the input electron beam power can be extremely high while the power density can be kept moderately low. The usual limitations on beam power imposed by space charge effects can therefore be overcome. Since the wave-particle interaction is fairly efficient (~50%), high radiation power levels can be achieved. The operating frequency is limited solely by the external magnetic field and is independent of the dimensions of any physical structure. Favorable coupling between the electrons and radiation field occurs near harmonics of the relativistic cyclotron frequency.

A quasioptical resonator has many modes which in principle can experience gain, producing a multimode output signal. The fundamental transverse resonator mode can be preferentially excited in

the open resonator. If the mirrors in the open resonator are made large enough to intercept a large fraction of the flux in the fundamental mode, we may expect this mode to have a large Q. The higher order modes can be expected to have a substantially smaller Q since they suffer from diffraction losses. This is an advantage over a closed cavity, where all modes would have comparable values of Q. Longitudinal modes in resonance within the resonator can undergo gain and produce a multimode output signal, unless they are suppressed. Longitudinal mode selection can be achieved by employing a mode selection; one such selector is the Smith-Fox interferometer.[26]

This new maser configuration, like the conventional electron cyclotron maser (gyrotron), has a wide range of practical applications. These applications range from electron cyclotron heating of fusion plasmas to advanced radar and communications systems. Because of the high field level, short wavelength, and extended interaction volume, the quasioptical maser may be a natural electromagnetic pump source for a free electron laser. In this application a second highly relativistic electron beam propagating along the axis of the open resonator would interact with the resonator field and induce high-frequency radiation. The frequency of the scattered radiation would be $\sim 4\gamma_y^2\omega$, where γ_y is the longitudinal gamma factor of the second relativistic electron beam and ω is the frequency of the quasioptical maser.

The possibility of ECM interaction in the open-resonator configuration of Fig. 1 has been pointed out in Ref. 27. The analysis and results of that work have several significant limitations, making a comparison with our work impossible. Most important among these limitations in Ref. 27 are the following: (a) The resonator fields are assumed to have no spatial dependence in the direction of the beam propagation. Such fields cannot be realized in practice. Our analysis is based on the realistic Gaussian spatial variation of the field amplitude. (b) The mildly relativistic limit is considered. Associated with this assumption are inaccuracies, which are avoided in our fully relativistic treatment. (c) The linear theory and the possibility of efficiency enhancement are not investigated.

II. NONLINEAR ANALYSIS OF QUASIOPTICAL MASER

The quasioptical cyclotron-maser configuration is depicted in Fig. 1. The lowest-order mode is the well known TEM_{00} Gaussian radiation beam (see Fig. 2). For the electric field vector primarily polarized in the x direction, the field components of this mode are

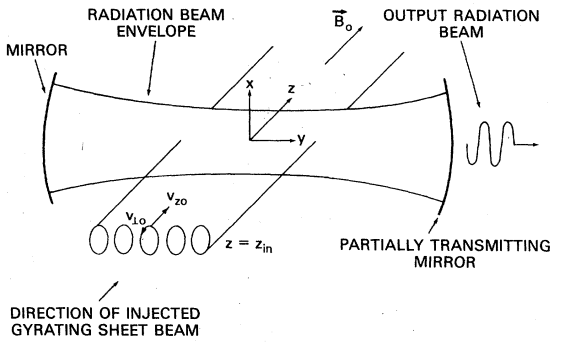

FIG. 1. Schematic representation of the quasioptical cyclotron maser. The electron beam propagates along and rotates about the z axis and the radiation beam axis coincides with the y axis.

$$E_x(x,y,z,t) = E(x,y,z)\sin[k_y y + \alpha(x,y,z)]\cos\omega t, \tag{1a}$$

$$B_z(s,y,z,t) = E(x,y,z)\cos[k_y y + \alpha(x,y,z)]\sin\omega t, \tag{1b}$$

where $k_y = \omega/c$, $E(x,y,z) = E_0(r_0/r_s(y))\exp[-(x^2+z^2)/r_s^2(y)]$, $\alpha(x,y,z) = R^{-1}(y)(x^2+z^2)(\omega/c)/2 - \tan^{-1}(y/y_R)$, ω is the radiation frequency, E_0 is the field amplitude at the origin, r_0 is the minimum spot size at the plane $y=0$, $r_s(y) = r_0(1+y^2/y_R^2)^{1/2}$ is the spot size at the plane y, $y_R = r_0^2\omega/2c$ is the Rayleigh length and $R(y) = y(1+y_R^2/y^2)$ is the radius of curvature of the spherical wave front at y. The y components of the field are $E_y = -(c/\omega)\partial E_x/\partial x$ and $B_y = -(c/\omega)\partial B_z/\partial z$. Note that $|E_y|, |B_y| \ll |E_x|, |B_z|$. One can show that the $\vec{E}$ and $\vec{B}$ fields satisfy the appropriate boundary conditions on the mirror. This is equivalent to saying that the mirror radius of curvature equals the wave-front radius of curvature.

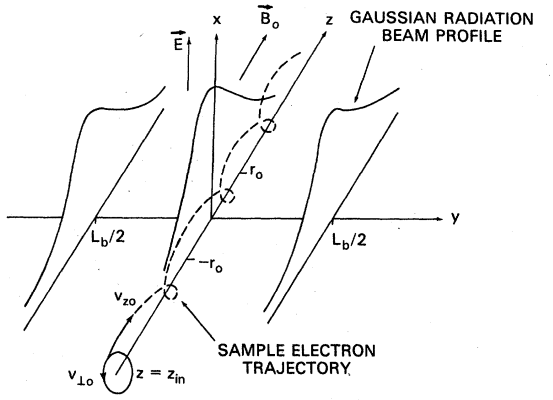

FIG. 2. Schematic representation of the trajectory of a sample electron as it crosses the radiation beam. The width of the electron beam is L_b.

The intermode frequency spacing is $\delta\omega = \pi c/L$ where L is the separation between the mirrors and the diffraction angle of the radiation is $\theta_d = \lambda/\pi r_0$ where $\lambda = 2\pi c/\omega$ is the radiation wavelength.

Other orientations of the external magnetic field and, hence, the gyrating electric beam are possible. Careful analysis, however, shows that these other configurations may not be as straightforward to implement. For example, another possible configuration is where the magnetic field and the streaming electrons are directed along the y axis. It can be shown that to maintain wave-particle coherence the thermal spread in the y component of electron velocity must satisfy $\delta v_y/v_y \ll \lambda/2\pi L$. For long resonators this condition places a rather stringent requirement on the electron-beam quality.

In Fig. 1, the gyrating beam electrons rotate in the x-y plane and stream along the external magnetic field $\vec{B}_0$ which is directed along the z axis. For convenience we locate the sheet electron beam of width L_b on the y-z plane, as shown in Fig. 1. Furthermore, for reasons of analytic simplicity, we take the guiding centers of the electrons, upon entering the resonator fields, to lie on the y-z plane. Also the electrons, upon entering the resonator, are assumed to have the same transverse and parallel velocities.

Strong coupling between the electrons and resonator field will occur at frequencies near multiples of the relativistic electron cyclotron frequency. Let us consider the fundamental cyclotron interaction, $\omega \approx \Omega_0/\gamma$ where $\Omega_0 = |e|B_0/m_0c$, $\gamma = (1+\vec{p}\cdot\vec{p}/m_0^2c^2)^{1/2}$, and $\vec{p}$ is the electron momentum vector. The electron Larmor radius is in general much less than the radiation wavelength, i.e., $r_L = \gamma v_\perp/\Omega_0 \approx \beta_\perp \lambda/2\pi \ll \lambda$, where $v_\perp = c\beta_\perp$ is the transverse electron velocity. The minimum radiation spot size is much greater than the Larmor radius, $r_0 > \lambda \gg r_L$. Therefore, by choosing the width of the electron beam to be somewhat less than the Rayleigh length, $L_b < y_R$, the resonator fields in (1) felt by the electrons can be accurately approximated by the plane-wave fields,

$$E_x(y,z,t) = E(z)\sin\left(\frac{\omega}{c}y\right)\cos(\omega t), \tag{2a}$$

$$E_y(y,z,t) = E(z)\cos\left(\frac{\omega}{c}y\right)\sin(\omega t), \tag{2b}$$

where $E(z) = E_0\exp(-z^2/r_0^2)$ and $E_y = B_y \approx 0$.

We now express the particle momenta $\vec{p}$ and transverse position (x,y) as functions of Lagrangian independent variables. In general, a convenient set of Lagrangian independent variables for this problem is the z position of the particles, the initial momentum-space angle Θ_0, initial transverse coordinates of the guiding center x_{go} and y_{go} and the particle entrance time into the resonator field t_0. Since the resonator fields fall off as $\exp(-z^2/r_0^2)$, the entrance position of the sheet beam z_{in} can be taken to be a few spot sizes away from the y axis, $|z_{in}| \gg r_0$. In our present analysis, $x_{go} = 0$, $|y_{go}| \leq L_b$ and t_0 is the time the particle crosses the $z = z_{in}$ plane. The functional dependence of the particle momenta vector and transverse coordinates is $\vec{p} = \vec{p}(z, y_{go}, \Theta_0, t_0)$, $x = x(z, y_{go}, \Theta_0, t_0)$, and $y = y(z, y_{go}, \Theta_0, t_0)$.

The orbit equations for the electrons are

$$p_z\frac{dp_x}{dz} = -|e|\left(\gamma m_0 E_x + \frac{p_y(B_0+B_z)}{c}\right), \tag{3a}$$

$$p_z\frac{dp_y}{dz} = |e|p_x(B_0+B_z)/c, \tag{3b}$$

$$\frac{dp_z}{dz} = 0, \tag{3c}$$

where the fields E_x and B_z are given by (2), with t replaced by the Lagrangian time variable

$$\tau(z, y_{go}, \Theta_0, t_0) = t_0 + \int_{z_{in}}^{z} dz'/v_z$$

and

$$v_z = p_z(z, y_{go}, \Theta_0, t_0)/\gamma(z, y_{go}, \Theta_0, t_0)m_0$$

is the longitudinal particle velocity. Note that p_z is a constant of the motion denoted by p_{zo}, hence, $v_z \neq 0$ unless $p_{zo} = 0$. The Lagrangian time variable τ is the time it takes a particle to arrive at z if it crossed the $z = z_{in}$ plane at time t_0 with a momentum-space angle Θ_0 and guiding center position $(x_{go} = 0, y_{go} = 0)$. Since we are considering only the fundamental cyclotron interaction, an appropriate representation of the solutions of the orbit equations in (3) are

$$p_x(z) = p_{xg}(z) + p_\perp(z)\cos(\omega\tau + \Theta), \tag{4a}$$

$$p_y(z) = p_{yg}(z) + p_\perp(z)\sin(\omega\tau + \Theta), \tag{4b}$$

where p_{xg}, p_{yg} are the components of momenta associated with the guiding centers, $p_\perp$ is the transverse particle momentum, and $\omega\tau + \Theta$ is the particle-momentum-space angle. In (4) the dependent variables p_{xg}, p_{yg}, $p_\perp$, and Θ are assumed to be slowly varying functions of z as well as functions of y_{go}, Θ_0, and t_0. By "slowly varying" we mean that the quantity has no high- (cyclotron) frequency Fourier components. The variables p_{xg}, p_{yg}, $p_\perp$, and Θ are not functionally independent of each other. In fact, by requiring that they be

slowly varying functions of z, we will derive four separate but coupled equations which uniquely determine them. The field amplitude $E(z)$ defined in Eq. (2) denotes the profile of the radiation beam and is a slowly varying function of z since the electrons undergo many cyclotron orbits while traversing the resonator fields. The initial values of dependent variables upon entering the open-resonator fields are $p_{xg}(z=z_{in})=p_{yg}(z=z_{in})=0$, $p_\perp(z=z_{in})=p_{\perp 0}$, $v_z(z=z_{in})=v_{z0}=p_{z0}/\gamma_0 m_0$, and $\Theta(z=z_{in})=\Theta_0$. Furthermore, it will be shown that the guiding center drift momentum of the particles is much less than the transverse momentum, i.e., $|p_{xg}|, |p_{yg}| \ll p_\perp$. Noting the form for p_y in (4b), we see that the dependent variable y can be approximated by

$$y = y_g - \frac{p_\perp}{m_0\Omega_0}\cos(\omega\tau+\Theta), \tag{5}$$

where y_g is the slowly varying y position of the guiding center, hence, $p_{yg}=p_{z0}dy_g/dz$ and $p_\perp/m_0\Omega_0 = r_L$ is the electron Larmor radius.

We now substitute (4a) and (4b) together with (5) into the orbit equations (3a) and (3b) and carry out the appropriate operations. Keeping in mind that $E(z)$ is a slowly varying function of z we equate rapidly varying terms and slowly varying terms and discard all frequencies of order $2\Omega_0$. These manipulations yield four interrelated self-consistent nonlinear equations describing the spatial evolution of $p_\perp$, Θ, p_{xg}, and p_{yg}. When $r_L \ll \lambda$, these equations are

$$\frac{dp_\perp}{dz} = \frac{-|e|E\gamma m_0}{2p_{z0}}\left[\sin\left(\frac{\omega}{c}y_g\right)\cos\Theta + \cos\left(\frac{\omega}{c}y_g\right)\left(\frac{p_{xg}}{m_0c}\cos\Theta + \frac{p_{xg}}{m_0c}\sin\Theta\right)\right]. \tag{6a}$$

$$\frac{d\Theta}{dz} = (\Omega_0-\gamma\omega)m_0/p_{z0} + \frac{|e|E\gamma m_0}{2p_{z0}p_\perp}\left[\sin\left(\frac{\omega}{c}y_g\right)\sin\Theta - \cos\left(\frac{\omega}{c}y_g\right)\left(\frac{p_{xg}}{m_0c}\sin\Theta - \frac{p_{yg}}{m_0c}\cos\Theta\right)\right], \tag{6b}$$

$$p_{xg} = \frac{|e|Ep_\perp}{2\Omega_0 m_0 c}\cos\left(\frac{\omega}{c}y_g\right)\sin\Theta, \tag{6c}$$

$$p_{yg} = \frac{|e|Ep_\perp}{2\Omega_0 m_0 c}\left(1-\frac{\omega\gamma}{\Omega_0}\right)\cos\left(\frac{\omega}{c}y_g\right)\cos\Theta, \tag{6d}$$

where $dy_g/dz = p_{yg}/p_{z0}$ and $\gamma=[1+(p_{z0}^2+p_\perp^2)/m_0^2c^2]^{1/2}$. Equations (6) completely describe the nonlinear steady-state particle dynamics for the fundamental cyclotron interaction. Since $|E/B_0| \ll 1$, it is noted from (6c) and (6d) that $|p_{xg}|, |p_{yg}| \ll p_\perp$, justifying the corresponding earlier assumption. The trajectory of each electron is described by the set of equations in (6). The initial conditions, however, are different for each electron, as required by the input distribution. For an entering cold unbounded electron beam, the initial conditions are such that at $z=z_{in}$, $p_{xg}=0$, $p_{yg}=0$, $p_\perp=p_{\perp 0}$, $p_z=p_{z0}$, $\Theta=\Theta_0$, where Θ_0 ranges from 0 to 2π, and $y_g=y_{go}$, where y_{go} ranges from $-L_b/2$ to $L_b/2$, while $p_{\perp 0}$ and p_{z0} are the same for all electrons.

The equations in (6) can be considerably simplified by noting from (6c) and (6d) that $p_{xg}/m_0c \simeq O(\gamma v_\perp E/2B_0) \ll 1$ and $p_{yg}/m_0c \approx O(p_{xg}\Delta\omega/m_0c\omega)$. Hence, the second and third terms in the brackets on the right-hand side of (6a) and (6b) can be neglected and y_g in (6a) and (6b) can be replaced by y_{go}. The resulting equations are

$$\frac{dp_\perp}{dz} = -\frac{|e|E\gamma m_0}{2p_{z0}}\sin\left(\frac{\omega}{c}y_{go}\right)\cos\Theta, \tag{7a}$$

$$\frac{d\Theta}{dz} = \frac{(\Omega_0-\gamma\omega)m_0}{p_{z0}} + \frac{|e|E\gamma m_0}{2p_{z0}p_\perp}\sin\left(\frac{\omega}{c}y_{go}\right)\sin\Theta. \tag{7b}$$

These equations are very similar to those analyzed in our initial studies[15] of the nonlinear behavior of the cyclotron-maser instability.

In a temporal steady-state oscillator the efficiency of converting beam power to radiation power is given by

$$\eta = (P_{b,in} - P_{b,out})/P_{b,in}, \tag{8}$$

where $P_{b,in}$ and $P_{b,out}$ is the total electron beam power flowing into and out of the open resonator in the z direction. For the cold beam distribution presented earlier, the efficiency, as defined in (8), can be shown to give

$$\eta = \frac{-|e|}{\gamma_0(\gamma_0-1)v_{z0}m_0^2c^2}\int_{z=z_{in}}^{z=z_{out}} dz \int_0^{2\pi/\omega}\frac{dt_0}{2\pi/\omega}\int_{-L_b/2}^{L_b/2}\frac{dy_{g0}}{L_b}\int_0^{2\pi}\frac{d\Theta_0}{2\pi}E_x p_x. \tag{9}$$

Using (2a) and (4a) we find that

$$E_x p_x = \frac{E p_\perp}{2} \sin\left(\frac{\omega}{c} y_{go}\right) \cos\Theta \,, \tag{10}$$

where we have used the approximations $y \approx y_{go}$ and $p_{xg} \approx 0$. Substituting (10) into (9) and noting that $E_x p_x$ is independent of t_0 we obtain for the efficiency the expression

$$\eta = \frac{-|e|\omega}{4\pi\gamma_0(\gamma_0 - 1)v_{zo}m_0^2c^2} \int_{z=z_{in}}^{z=z_{out}} dz \int_{-L_b/2}^{L_b/2} \frac{dy_{go}}{L_b} \int_0^{2\pi} \frac{d\Theta_0}{2\pi} E(z) p_\perp(z, \Theta_0, y_{go}) \sin\left(\frac{\omega}{c} y_{go}\right) \cos\Theta(z, \Theta_0, y_{go}) . \tag{11}$$

The expression in (11) gives the full nonlinear steady-state operating efficiency. Before solving (11) in the fully nonlinear regime it is illuminating to first solve the orbit equations in the linear regime and thereby obtain the analytic form for the efficiency. The orbit equation in (7) can be linearized by setting $p_\perp = p_\perp^{(0)} + p_\perp^{(1)}$ and $\Theta = \Theta^{(0)} + \Theta^{(1)}$, where $p_\perp^{(0)}$ and $\Theta^{(1)}$ are zero-order quantities in the field amplitude E, and $p_\perp^{(1)}$ and $\Theta^{(1)}$ are first-order quantities. Solving (7) we find that

$$p_\perp^{(0)} = p_{\perp 0} \,, \tag{12a}$$

$$\Theta^{(0)}(z) = \Theta_0 - \frac{\Delta\omega}{v_{zo}}(z - z_{in}) \,, \tag{12b}$$

$$p_\perp^{(1)} = \frac{-|e|}{2v_{zo}} \sin\left(\frac{\omega}{c} y_{go}\right) \int_{z_{in}}^{z} dz' \, E(z') \cos\Theta^{(0)} \,, \tag{12c}$$

$$\Theta^{(1)} = \frac{|e|}{2v_{zo}} \frac{v_{\perp 0}\omega}{p_{zo}c^2} \sin\left(\frac{\omega}{c} y_{go}\right) \int_{z_{in}}^{z} dz' \int_{z_{in}}^{z'} dz'' \, E(z'') \cos\Theta^{(0)}(z'') + \frac{1}{p_{\perp 0}} \frac{\partial p_\perp^{(1)}}{\partial \Theta_0} \,, \tag{12d}$$

where $\Delta\omega = \omega - \Omega_0/\gamma_0$ is the frequency mismatch.

Now substituting (12) into (11) and performing the y_{go} integration we arrive at the following expression for the linear efficiency:

$$\eta = \frac{-(|e|/m_0c^2)^2}{8\beta_{zo}^2\gamma_0(\gamma_0 - 1)} \int_{z_{in}}^{z_{out}} dz \int_z^z dz' \left[E(z)E(z') \cos\left(\frac{\omega}{c}(z' - z)\frac{\Delta\omega/\omega}{\beta_{zo}}\right) + \frac{\omega/c}{2\beta_{zo}} \beta_{\perp 0}^2 \int_z^{z'} dz'' \, E(z)E(z'') \sin\left(\frac{\omega}{c}(z'' - z)\frac{\Delta\omega/\omega}{\beta_{zo}}\right) \right] , \tag{13}$$

where $E(z)$ denotes the profile of the radiation beam. In the present case the radiation beam has a Gaussian profile given by $E(z) = E_0 \exp(-z^2/r_0^2)$. Substituting this form for $E(z)$ into (13) and taking the beam entrance and exit planes to be, respectively, $z_{in} = -\infty$ and $z_{out} = \infty$, the integrations over z, z', and z'' can be performed analytically. The overall expression for the linear, small-signal efficiency takes the rather simple form

$$\eta = \frac{\pi}{16} \frac{\gamma_0}{\gamma_0 - 1} \left(\frac{E_0}{B_0}\right)^2 \xi_0^2 \exp\left[-\tfrac{1}{2}\left(\xi_0 \frac{\Delta\omega}{\omega}\right)^2\right] \left(\frac{\beta_{\perp 0}^2}{2} \xi_0^2 \frac{\Delta\omega}{\omega} - 1\right), \tag{14}$$

where $\xi_0 = (r_0\omega/c)/\beta_{zo}$. Unlike the case of a beam propagating along the z axis, the structure of η is nonoscillating in, say, r_0. The reason for this is that the radiation field is a smooth function of z and has no abrupt change in behavior at the entry and exit points of the electrons. From (14) we see that the efficiency is positive when $\Delta\omega/\omega > 2/\beta_{\perp 0}\xi_0)^2$, hence, the output frequency is always slightly higher than the relativistic cyclotron frequency. For typical choices of parameters, the term $\beta_{\perp 0}^2 \xi_0^2 (\Delta\omega/\omega)/2$ is much greater than unity. In this case the linear efficiency maximizes when the frequency shift is $\Delta\omega = \omega/\xi_0$.

Appendix A contains a derivation of the small-signal efficiency at the fundamental as well as at all cyclotron harmonics using the linearized Vlasov equation. In this appendix the linear-efficiency expression is derived for the cases where the electric field of the radiation beam is polarized in the x direction, i.e., polarization considered in the body of this paper, as well as in the z direction. The former polarization of the electric field is shown to result in substantially higher linear efficiencies compared to the latter polarization. In conventional electron cyclotron masers the particle interacts with the TE mode of the structure. This corresponds, in our present configuration, to the electric field polarized in the x direction. Polarization of the electric field in the z direction would correspond to a TM mode interaction in the conventional configuration.

In order for the system to operate in the as-

sumed steady state, there must be losses which just compensate for the power loss of the electron beam. These losses are composed of both the output radiated power, and the real losses due to diffraction or dissipation in the mirrors. All of these losses are characterized by the Q of the cavity so that the total power out of the resonator is $P_{\text{out}}=\omega\mathcal{E}_{\text{stored}}/Q$, where $\mathcal{E}_{\text{stored}}$ is the energy stored in the cavity, which is proportional to E_0^2. Since linear theory shows that power lost by the beam is also proportional to E_0^2, the operating field amplitude cannot be determined by linear theory alone. Thus, the oscillator, unlike the amplifier, is an inherently nonlinear device.

As will be shown in Sec. III, where the nonlinear electron dynamics are calculated, the power lost by the beam ultimately levels off as E_0^2 increases. Thus the actual operating point can be calculated from the intersection of the graphs of power loss by the beam, and power lost by the cavity, as functions of E_0^2, shown schematically in Fig. 3. It is apparent that the steady state can be achieved only if the losses are small enough so that the two curves intersect. Also, for the optical cavity configuration, we find that the power lost by the beam never becomes negative as E_0^2 increases. Thus steady-state operation is not possible without power loss by the cavity.

The threshold condition for starting the oscillations in the resonator is

$$\eta P_{b,\text{in}} \geq \omega\mathcal{E}_{\text{stored}}/Q\,, \tag{15}$$

where $\mathcal{E}_{\text{stored}}=\frac{1}{4}(E_0^2/8\pi)\pi r_0^2 L$ is the stored field energy. To obtain the threshold electron-beam power, necessary to start the resonator, we use the small-signal efficiency in Eq. (14). Substituting the maximum small-signal efficiency, i.e., when $\xi_0\Delta\omega/\omega=1$, into (15) we find that the product of the beam power and resonator Q needed to start the oscillations is

$$P_{b,\text{in}}Q \geq 4.6\times10^9\frac{L}{r_0}\gamma_0(\gamma_0-1)\beta_{z0}^3/\beta_{\perp0}^2(\text{watts})\,. \tag{16}$$

Throughout our analysis on the quasioptical maser we have made the tacit assumption that the energy lost by the electrons goes into supporting the assumed Gaussian radiation beam. This assumption is common to all conventional oscillator problems and has been proven valid experimentally. Although we have not rigorously proven this point, concerning our present configuration, we have assumed it applies here too.

III. NUMERICAL RESULTS AND ILLUSTRATIONS

A. Efficiency of maser in uniform external magnetic field

As an illustration of the potential operation of the quasioptical maser we choose a 60-keV ($\gamma_0=1.118$) electron beam having initial velocity components $\beta_{\perp0}=0.4$ and $\beta_{z0}=0.2$. The location and curvature of the mirrors are chosen so that the radiation spot size is 5.9 wavelengths, i.e. $r_0=5.9\lambda$. The linear (small-signal) efficiency given by (14) is shown in Fig. 4 for various values of the normalized field amplitude, E_0/B_0. The linear efficiency has a single positive maximum when $\xi_0\Delta\omega/\omega=1$ which corresponds to the frequency $\omega_{\max}=(1-1/\xi_0)^{-1}\Omega_0/\gamma_0$. The intermode frequency separation of a resonator of length L is $\delta\omega=\pi c/L$. Therefore, a spectrum of natural modes can exist within the resonator separated in frequency by $\delta\omega$. When the oscillator is first started up, the mode frequency closest to $\omega_{\max}$ will be excited first and grow to a level where it suppresses the slower growing natural modes further away from $\omega_{\max}$. It turns out that the maximum nonlinear efficiency occurs at a frequency slightly higher than $\omega_{\max}$, i.e., for $\xi_0\Delta\omega/\omega$ somewhat larger than unity.

In the absence of longitudinal mode selection or equivalent scheme, it would not be possible to take

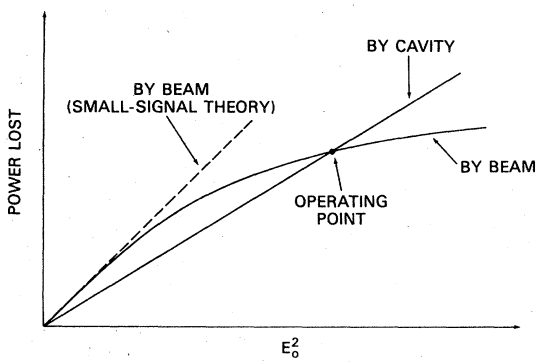

FIG. 3. Determination of the point of nonlinear steady-state operation.

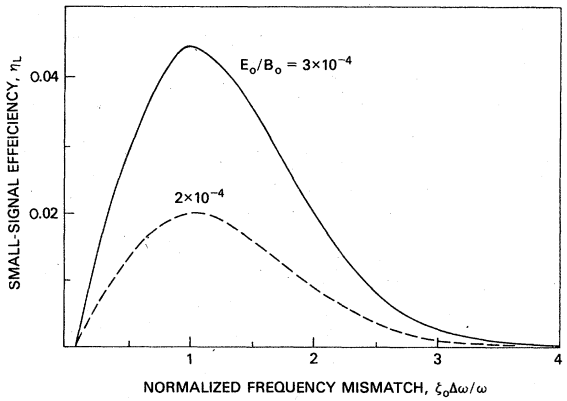

FIG. 4. Linear efficiency η_L vs normalized frequency mismatch $\xi_0\Delta\omega/\omega$ for $\beta_{\perp0}=0.4$, $\beta_{z0}=0.2$, and $r_0/\lambda=5.9$.

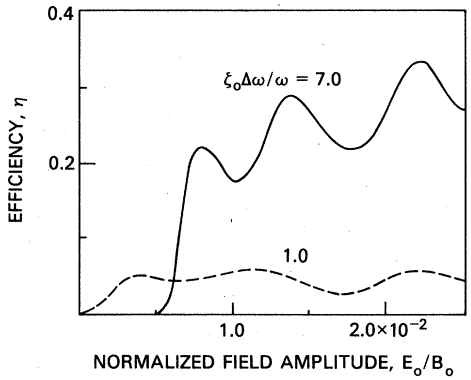

FIG. 5. Nonlinear efficiency η vs normalized field amplitude E_0/B_0 at the frequency mismatch of optimal (a) nonlinear operation $\xi_0\Delta\omega/\omega=7.0$ (solid line) and (b) linear operation $\xi_0\Delta\omega/\omega=1.0$ (dashed line). The other parameters are the same as in Fig. 4.

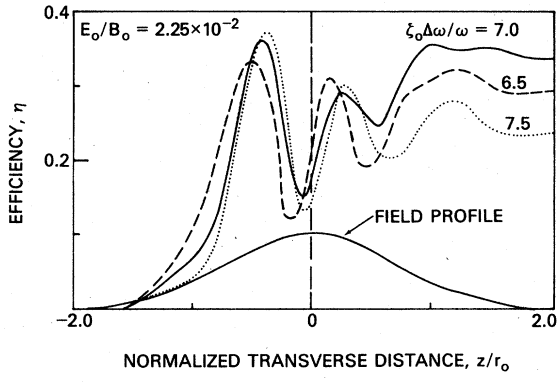

FIG. 6. Spatial variation of the nonlinear efficiency η across the resonator for the parameters of Fig. 4 at the optimal nonlinear point, $E_0/B_0=2.25\times10^{-2}$ and $\xi_0\Delta\omega/\omega=7.0$ (solid line), as well as for $\xi_0\Delta\omega/\omega=6.5$ (dashed line) and $\xi_0\Delta\omega/\omega=7.5$ (dotted line). The radiation field profile is shown for reference on an arbitrary scale.

advantage of the higher nonlinear efficiencies occurring at frequencies greater than ω_{max}. To suppress these unwanted modes near ω_{max} and operate the maser at the frequency of maximum nonlinear efficiency, we will assume that a longitudinal mode selector[26] is employed. Another approach seems possible: we can start the oscillator at the natural operating frequency ω_{max}. When the mode saturates, the external magnetic field can be decreased slightly so that $\xi_0\Delta\omega/\omega\gtrsim1$ has the appropriate value to maximize the nonlinear efficiency. We will assume that, by using either of these approaches, the operating frequency can be freely chosen.

The nonlinear efficiency defined in Eq. (11) is evaluated by following numerically the particle trajectories according to (6). For sufficiently small field amplitudes, the simulations reproduce very accurately the linear efficiency in (13). The beam entry and exit points were taken at $\pm2r_0$ and the electron orbits were integrated using a four-point Runge-Kutta integrator. Figure 5 demonstrates the higher nonlinear efficiencies achievable at larger values of $\xi_0\Delta\omega/\omega$. The efficiency in this figure is obtained by solving (11) as a function of E_0/B_0 for various values $\xi_0\Delta\omega/\omega$. A maximum efficiency of 33% is obtained for $\xi_0\Delta\omega/\omega=7$ at $E_0/B_0=2.25\times10^{-2}$. Figures 6 and 7 show the spatial variation of the efficiency within the resonator for various values of the normalized frequency shift $\xi_0\Delta\omega/\omega$ and normalized field amplitude E_0/B_0. The spatial oscillations in efficiency within the resonator are due to the oscillations of the trapped particle distribution. The Gaussian profile of the radiation beam is also shown in Fig. 6 for reference purposes.

The examples presented so far should not lead to the impression that good performance is necessarily associated with frequency mismatches significantly larger than the values corresponding to maximum linear gain. For example, for a beam with $\beta_{\|0}=0.1$ and $\beta_{\perp0}=0.2$, corresponding to $\gamma_0=1.026$ (13.3 keV), the nonlinear efficiency is plotted in Fig. 8 against the radiation field amplitude for various values of the ratio r_0/λ. In all cases the frequency mismatch was taken to correspond to the *maximum linear gain value*, obtained from Eq. (14). As can be seen in Fig. 8, a peak efficiency of 20% is obtained for $r_0/\lambda=2.5$, while the values of $\eta=17.5\%$ are obtained for $r_0/\lambda=1.6$ and 3.2. For these cases, the frequency mismatch is given by $\Delta\omega/\omega=0.75\times10^{-2}$, 1.30×10^{-2}, and 0.58×10^{-2}, respectively, and corresponds to optimal linear gain value.

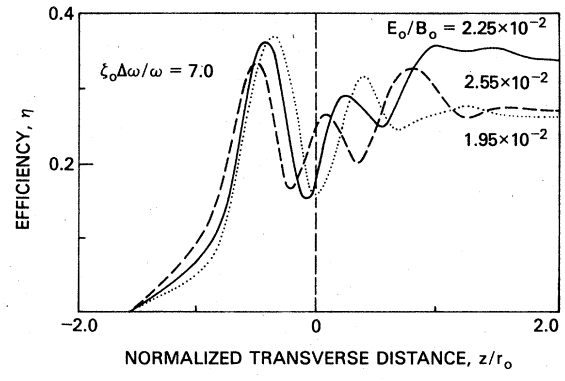

FIG. 7. Spatial variation of the nonlinear efficiency η across the oscillator for the parameters of Fig. 4 at the optimal nonlinear point, $\xi_0\Delta\omega/\omega=7.0$ and $E_0/B_0=2.25\times10^{-2}$ (solid line), as well as for $E_0/B_0=2.55\times10^{-2}$ (dashed line) and $E_0/B_0=1.95\times10^{-2}$ (dotted line).

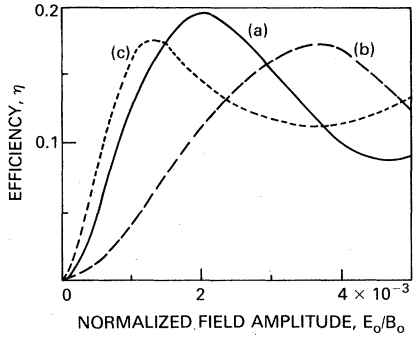

FIG. 8. Nonlinear efficiency η vs normalized field amplitude E_0/B_0 for $\beta_{\perp 0}=0.2$ and $\beta_{z0}=0.1$ for operation at the point of optimal linear operation, when (a) $r_0/\lambda=2.5$, $\Delta\omega/\omega=0.75\%$ (solid line), (b) $r_0/\lambda=1.6$, $\Delta\omega/\omega=1.30\%$ (dashed line), and (c) $r_0/\lambda=3.2$, $\Delta\omega/\omega=0.58\%$ (dotted line).

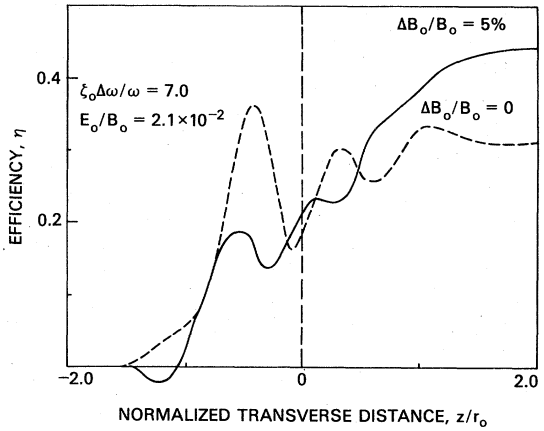

FIG. 9. Spatial evolution of the nonlinear efficiency η across the oscillator for the parameters of Fig. 4 and for $\xi_0\Delta\omega/\omega=7.0$ and $E_0/B_0=2.1\times10^{-2}$, (a) when the external magnetic field is decreased by 5% over the distance $4r_0$ (solid line) and (b) when the external magnetic field is uniform (dashed line).

B. Efficiency enhancement by contouring external magnetic field

It is possible to enhance the nonlinear operating efficiency of the quasioptical maser by either prebunching the electron beam in momentum-phase angle $(\omega\tau-\Theta)$ or by appropriately contouring the external magnetic field. Prebunching the electron beam, by utilizing a two-open-resonator Klystron-type configuration, is in principle straightforward and results in extremely high efficiencies. However, depending on the length of the ballistic phase-bunching region (distance between the two resonators), electron-beam thermal effects may present a problem at high frequencies. Contouring the magnetic field appears to be the simplest method for enhancing efficiency. By slightly contouring the magnetic field, as a function of z, a more advantageous momentum-phase distribution of the electrons can be realized with a single resonator. A significant improvement in efficiency over the already highly efficient uniform magnetic field case can be realized in this way. Figure 9 shows the spatial evolution of efficiency with and without magnetic field contouring. The magnetic field in this case was decreased linearly by 5% between the points $z=-2r_0$ and $z=2r_0$. For this variation a final total efficiency of 45% was achieved.

C. Design examples

We conclude with two specific detailed design examples, which will demonstrate the potential of the configuration we have analyzed. In the following examples the steady-state performance of the maser, operating at 150 GHz ($\lambda=2$ mm), is analyzed. The electron beam is taken to be generated by a diode with a current density of 10 A/cm^2. Within the oscillator, the electron beam has a rectangular cross section,[28] with area $A=2r_0y_R$, extending from $x=-r_0/2$ to $x=+r_0/2$ and from $y=-y_R$ to $y=+y_R$, where r_0 is the spot size and y_R is the Rayleigh length.

The first example deals with the 60-keV beam with $\beta_{\perp 0}=0.4$ and $\beta_{\parallel}=0.2$, for which the efficiency is shown in Fig. 5. For $r_0/\lambda=5.9$, the beam cross section is $A=52$ cm^2, giving a beam current of 520 A and an input beam power of 31 MW. Owing to the slight variations of the radiation field amplitude across the beam, the conversion efficiency has to be appropriately averaged. For a radiation field of magnitude $E_0/B_0=2.4\times10^{-2}$ at the center of the beam, this weighted average efficiency is $\eta=28\%$, hence the radiated output power is $P_{\rm rad}=8.7$ MW. For such performance, a normalized frequency mismatch $\xi_0\Delta\omega/\omega=7$ is required, hence $\Delta\omega/\omega=3.77\%$ and $\omega/\Omega_0=0.93$. For $\lambda=2$ mm ($\omega=9.4\times10^{11}$ sec^{-1}), a magnetic field of $B_0=58$ kG is required. In addition, by appropriately tapering the external magnetic field the output power can be increased to $P_{\rm rad}=12$ MW. Finally, if either of the above illustrations (with or without the external field taper) is to be achieved by initially adjusting the external magnetic field to the value corresponding to maximum linear gain of the operating frequency, then for a 44-cm-long resonator (i.e., equal to $2y_R$), the value of Q obtained from (16) must exceed the 180, while the operating value of Q is 40 000.

In the above example the frequency mismatch was substantially higher than the value required for maximum linear gain. The highly impressive

performance associated with the adoption of such a condition warrants its implementation. The realization of such a large frequency mismatch would require a mode selector or an external source to set up the radiation field. However, if such complications are to be avoided, excellent performance can be achieved as will be shown. In the second example we consider a 13.3-keV beam with $\beta_{\parallel 0}=0.1$ and $\beta_{\perp 0}=0.2$, interacting with a radiation beam of $\lambda=0.2$ cm and $r_0/\lambda=2.5$, at the frequency mismatch associated with maximum linear gain, i.e., $\Delta\omega/\omega=0.75\%$. In this case, the cross-sectional area of the beam is $A=4$ cm^2. Assuming that the diode current density of 10 A/cm^2 can be compressed to 50 A/cm^2, the input beam power is 2.7 MW. For $E_0/B_0=2.3\times10^{-3}$, the average efficiency is 18%, hence the radiation power is $P_{\rm rad}=0.50$ MW. The required value of the external magnetic field is $B_0=54.5$ kG. For this case, the linear threshold condition (16) is not restrictive, since it simply requires that the nonlinear efficiency be smaller than the linear value, which is the case. Assuming an oscillator length equal to 16 $y_R=63$ cm, the operating value Q is 1560, larger than the threshold value of 150, required by (16).

APPENDIX A

Here we work out the steady-state linear theory for the energy loss of the electron beam as it traverses the wave fields in the open resonator. In steady state, the energy equation for the beam is

$$\frac{\partial}{\partial z}W_{fl}=\vec{E}\cdot\vec{J}\,, \tag{A1}$$

where W_{fl} is the beam energy flux and $\vec{J}$ is the beam current. The configuration is as shown in Fig. 1. The change in beam power as it crosses the resonator then is $\int d^3r\,\vec{E}\cdot\vec{J}$, so the main problem is to calculate an expression for the perturbed beam current density $\vec{J}$.

This can most easily be done by analyzing the linearized Vlasov equation

$$\left(-i\omega+\vec{v}\cdot\vec{\nabla}-\frac{|e|\vec{p}\times\vec{B}_0}{\gamma m_0 c}\cdot\frac{\partial}{\partial\vec{p}}\right)f^{(1)} =|e|\left(\delta\mathbf{E}+\frac{\vec{p}\times\delta\vec{B}}{\gamma m_0 c}\right)\cdot\frac{\partial f^{(0)}}{\partial\vec{p}}\,, \tag{A2}$$

where a time dependence $e^{-i\omega t}$ is assumed. The quantity $f^{(0)}$ is the unperturbed distribution function, that is, the distribution function at $z=-\infty$, and $f^{(1)}$ is the perturbation to it induced by the fields in the resonator. Instead of using independent variables $\vec{r}$, $\vec{p}$, it is more convenient to use as independent variables the quantities $(x_g, y_g, z, p_\perp, \phi, p_z)$ where

$$\begin{aligned} p_x&=p_\perp\cos\left(\frac{\Omega_0 m_0}{p_z}z+\phi\right),\\ p_y&=p_\perp\sin\left(\frac{\Omega_0 m_0}{p_z}z+\phi\right), \end{aligned} \tag{A3}$$

and

$$\begin{aligned} x&=x_g+\frac{p_\perp\sin\left(\frac{\Omega_0 m_0}{p_z}z+\phi\right)}{\Omega_0 m_0},\\ y&=y_g-\frac{p_\perp\cos\left(\frac{\Omega_0 m_0}{p_z}z+\phi\right)}{m_0\Omega_0}, \end{aligned} \tag{A4}$$

where Ω_0 is the nonrelativistic cyclotron frequency. These have the advantage of being constant in the absence of the radiation fields in the resonator. In these new variables, the Vlasov equation reduces to

$$\left(-i\omega+\frac{p_z}{\gamma m_0}\frac{\partial}{\partial z}\right)f^{(1)}=|e|\left(\delta\vec{E}+\frac{\vec{p}\times\delta\vec{B}}{\gamma m_0 c}\right)\cdot\frac{\partial f^{(0)}}{\partial\vec{p}}\,, \tag{A5}$$

and assuming that $f^{(0)}$ is independent of ϕ, $\partial f^{(0)}/\partial\vec{p}$ reduces to

$$\frac{\partial f^{(0)}}{\partial p}=\left\{\hat{e}_x\left[2p_\perp\cos\left(\frac{\Omega_0 m_0}{p_z}z+\phi\right)\frac{\partial}{\partial p_\perp^2}+\frac{1}{\Omega_0 m_0}\frac{\partial}{\partial y_g}\right]+\hat{e}_y\left[2p_\perp\sin\left(\frac{\Omega_0 m_0}{p_z}z+\phi\right)\frac{\partial}{\partial p_\perp^2}-\frac{1}{\Omega_0 m_0}\frac{\partial}{\partial x_g}\right]+\hat{e}_z\frac{\partial}{\partial p_z}\right\}f^{(0)}\,. \tag{A6}$$

There are two possible polarization for the radiation. The first is

$$\begin{aligned} \delta\vec{E}&=E(z)\cos(ky)\,e^{-i\omega t}\hat{e}_x+\text{c.c.}\,,\\ \delta\vec{B}&=\frac{ikc}{\omega}E(z)\sin(ky)\,e^{-i\omega t}\hat{e}_z+\text{c.c.}\,, \end{aligned} \tag{A7}$$

which we call TE since it has $\delta\vec{E}\perp\vec{B}_0$. The second polarization

$$\begin{aligned} \delta\vec{E}&=E(z)\cos(ky)\,e^{-i\omega t}\hat{e}_z+\text{c.c.}\,,\\ \delta\vec{B}&=\frac{-ikc}{\omega}E(z)\sin(ky)\,e^{-i\omega t}\hat{e}_x+\text{c.c.} \end{aligned} \tag{A8}$$

is TM since $\delta\vec{B} \perp \vec{B}_0$.

For TE polarization, the linearized Vlasov equation reduces to

$$\left(\frac{\partial}{\partial z} - \frac{i\gamma m_0 \omega}{p_z}\right) f^{(1)} = \frac{\gamma m_0}{p_z} \frac{|e| E(z)}{2\omega} e^{i(ky-\omega t)} \left\{ 2\omega p_\perp \cos\left(\frac{\Omega_0 m_0 z}{p_z} + \phi\right) \frac{\partial}{\partial p_\perp^2} + \left[\omega - \frac{k p_\perp}{\gamma m_0} \sin\left(\frac{\Omega_0 m_0 z}{p_z} + \phi\right)\right] \frac{1}{\Omega_0 m_0} \frac{\partial}{\partial y_g} \right.$$
$$\left. - \frac{k p_\perp}{\gamma m_0} \frac{1}{\Omega_0 m_0} \cos\left(\frac{\Omega_0 m_0 z}{p_z} + \phi\right) \frac{\partial}{\partial x_g} \right\} f^{(0)} + (k \to -k) \equiv G(z) . \tag{A9}$$

The perturbed distribution function then is

$$f^{(1)} = \exp\left(i \frac{\gamma m_0 \omega z}{p_z}\right) \int_{-\infty}^{z} dz' \exp \frac{-i\gamma m_0 \omega z'}{p_z} G(z') . \tag{A10}$$

The quantity we are interested in is $\int \delta\vec{E}^* \cdot \delta\vec{J}\, d^3r$ which is

$$-|e| \int p_\perp dp_\perp dp_z d\phi\, dx_g dy_g dz\, (p_\perp/\gamma m_0) \cos(\Omega_0 m_0 z/p_z + \phi) \delta E^* f^{(1)} .$$

In evaluating this integral, $\exp(iky)$, which appears in the expression for $\delta\vec{E}$ must be written as $\exp\{ik[y_g - (p_\perp/\Omega_0 m_0)\cos(\Omega_0 m_0 z/p_z + \phi)]\}$ which is equal to

$$\sum_n J_n\left(\frac{k p_\perp}{\Omega_0 m_0}\right) \exp i\left[k y_g + n i\left(\frac{\pi}{2} \frac{\Omega_0 m_0 z}{p_z} + \phi\right)\right] .$$

Then $\int \vec{E}^* \cdot \vec{J}\, d^3r$ is given by

$$\int d^3r\, \vec{E}^* \cdot \vec{J} = \tfrac{1}{4} \int dx_g dy_g dz\, p_\perp dp_\perp d\phi\, dp_z E^*(z) \sum_{n'=-\infty}^{\infty} J_{n'}\left(\frac{k p_\perp}{\Omega_0 m_0}\right) \exp\left[-in'\left(\frac{\Omega_0 m_0 z}{p_z} + \phi - \frac{\pi}{2}\right)\right]$$
$$\times \int_{-\infty}^{z} dz' \exp\left(i \frac{\gamma m_0 \omega (z - z')}{p_z}\right) \left(\frac{-|e|^2}{\omega}\right)$$
$$\times E(z) \sum_{n=-\infty}^{\infty} J_n\left(\frac{k p_\perp}{\Omega_0 m_0}\right) \exp\left[in\left(\frac{\Omega_0 m_0 z}{p_z} + \phi - \frac{\pi}{2}\right)\right]$$
$$\times \frac{p_\perp}{p_z} \cos\left(\frac{\Omega_0 m_0 z'}{p_z} + \phi\right) \cos\left(\frac{\Omega_0 m_0 z}{p_z} + \phi\right) \left(2\omega p_\perp \frac{\partial f^{(0)}}{\partial p_\perp^2}\right)$$
$$+ (k \to -k) + \text{c.c.} , \tag{A11}$$

where we have assumed that $\partial f^{(0)}/\partial y_g = 0$, that is, the distribution of guiding centers is uniform in the y direction (actually the dimension of the beam in the y direction is very long compared to a wavelength), and also have exploited the fact that no quantity except $f^{(0)}$ depends on x_g, so the $\partial f^{(0)}/\partial x_g$ term integrates to zero. Since $f^{(0)}$ is independent of ϕ, the only term which does not integrate to zero over ϕ is the zero Fourier harmonic. This collapses the double summation over n and n' into a single summation, so that

$$\int d^3r\, \vec{E}^* \cdot \vec{J} = 2\pi |e|^2 \int dx_g dy_g dz\, p_\perp dp_\perp dp_z E^*(z) \sum_{n=-\infty}^{\infty} \left[J_n'\left(\frac{k p_\perp}{m_0 \Omega_0}\right)\right]^2 \int_{-\infty}^{z} dz' \exp\left[i\left(\frac{\gamma m_0 \omega}{p_z} - \frac{\Omega_0 m_0}{p_z}\right)(z - z')\right] \frac{p_\perp^2}{p_z} \frac{\partial f^{(0)}}{\partial p_\perp^2} + \text{c.c.} , \tag{A12}$$

where the $(k \to -k)$ has now been explicitly included.

The next problem is to evaluate the zz' integral. Assuming $E(z)$ has the form $E_0 \exp(-z^2/r_0^2)$, this integral is of the form

$$\int_{-\infty}^{\infty} dz \int_{-\infty}^{z} dz' \exp\left\{-\left[\left(\frac{z}{r_0}\right)^2 + \left(\frac{z'}{r_0}\right)^2 + i\alpha (z - z')\right]\right\}$$

where $\alpha = (\gamma m_0 \omega - n m_0 \Omega_0)/p_z$. By completing the square, the z' integral can be evaluated in terms of error functions so it reduces to a single integral

$$\frac{\sqrt{\pi}}{2} r_0^2 e^{-\alpha^2 r^2/2} \int_{-\infty}^{\infty} du \exp[-(u + i\alpha r_0)^2](1 + erfu) .$$

Since the error function is an odd function of u, the integral of the term containing the error function is

$$\int_{-\infty}^{\infty} -i\sin(2\alpha r_0 u)e^{-u^2} erf u\,,$$

which is purely imaginary and sums to zero upon adding the complex conjugate. Thus only the unity in the parentheses contributes to the integral and the total result is $\frac{1}{2}\pi r_0^2 \exp(-\alpha^2 r_0^2/2)$. Hence the total result is

$$\int d^3r\, \vec{E}^* \cdot \vec{J}\Big|_{TE} = -|e|^2 \frac{\pi^2}{2} \int dx_g dy_g dp_\perp^2 dp_z \sum_{n=-\infty}^{\infty} E_0^2 r_0^2 \exp\left\{-\left[\left(\frac{\gamma m_0\omega - n m_0\Omega_0}{p_z}\right)^2 \frac{r_0^2}{2}\right]\right\}\left[J_n'\left(\frac{kp_\perp}{\Omega_0 m_0}\right)\right]^2 \frac{p_\perp^2}{p_z}\frac{\partial f^{(0)}}{\partial p_\perp^2}\,. \tag{A13}$$

This is the final result for the power loss of the beam as it traverses the fields in the open resonator. To progress further, assume the distribution function

$$f^{(0)} = \frac{\sigma}{2\pi}\delta(p_\perp^2 - p_{\perp 0}^2)\delta(p_z - p_{z0})\delta(x_g)\,, \tag{A14}$$

where σ is the surface charge density of the sheet beam. The incident power is

$$W_{fl} = L\sigma(\gamma - 1)p_z c^2/\gamma\,. \tag{A15}$$

Assuming $n=1$, $\omega \simeq \Omega_0/\gamma$, and $J_1(x) \simeq x/2$ (i.e., $kp_\perp \ll \Omega_0 m_0$ the integrals can easily be done and Eq. (14) can be recovered for the efficiency. For $n=2$ one can also show that the efficiency has the same basic form as Eq. (14), but it is multiplied by an overall factor of $\frac{1}{4}(k^2 p_\perp^2/m_0^2\Omega_0^2)$, which is much less than unity. Thus an interaction at the second harmonic exists, but it is weaker.

For the TM mode an analogous calculation gives the result

$$\int d^3r\, \vec{E}^* \cdot \vec{J}\Big|_{TM} = -|e|^2 \frac{\pi^2}{2} \int dx_g dy_g dp_\perp^2 dp \sum_{n=-\infty}^{\infty} r_0^2 \exp\left[-\frac{r_0^2}{2}\left(\frac{\gamma m_0\omega - n m_0\Omega_0}{p_z}\right)\right]$$
$$\times E_0^2 J_n^2\left(\frac{kp_\perp}{\Omega_0 m_0}\right)\left[\frac{1}{2}\left(1 - \frac{n\Omega_0}{\gamma\omega}\right)\frac{\partial}{\partial p_z} + \frac{n\Omega_0}{\gamma m_0 p_z}\frac{\partial}{\partial p_\perp^2}\right] g\,. \tag{A16}$$

At each harmonic, the power loss of the beam is smaller by a factor of order $(kp_\perp/\Omega_0 m_0)^2$ from what it was for the same harmonic with TE polarization. Thus the coupling of the TM mode with the radiation in the optical cavity is much weaker than for the TE mode.

ACKNOWLEDGMENTS

This work has been supported by the U. S. Department of Energy under Project No. DE-AI01-80ER52065.

*Permanent address: JAYCOR, Alexandria, Virginia 22304.
[1]J. M. J. Madey, H. A. Schwettman, and W. M. Fairbrank, IEEE Trans. Nucl. Sci. 20, 980 (1973).
[2]P. Sprangle and V. L. Granatstein, Appl. Phys. Lett. 25, 377 (1974).
[3]W. B. Colson, Phys. Lett. A59, 187 (1976).
[4]T. Kwan, J. M. Dawson, and A. T. Lin, Phys. Fluids 20, 581 (1977).
[5]N. M. Kroll and W. A. McMullin, Phys. Rev. A 17, 300 (1978).
[6]A. Gover and A. Yariv, Appl. Phys. 16, 121 (1978).
[7]P. Sprangle, Cha-Mei Tang, and W. M. Manheimer, Phys. Rev. Lett. 43, 1932 (1979).
[8]P. Sprangle and R. A. Smith, Phys. Rev. A 21, 293 (1980).
[9]N. M. Kroll, P. Morton, and M. N. Rosenbluth, JASON Tech. Report No. JSR-79-15, 1980 (unpublished).
[10]R. Q. Twiss, Aust. J. Phys. 11, 564 (1958).
[11]A. V. Gaponov, Izv. Vyssh. Uchebn. Zaved. Radiofiz. 2, 450 (1959); and 2, 836 (1959).
[12]R. H. Pantell, Proc. IRE 47, 1146 (1959).
[13]M. Borenstein and W. E. Lamb, Jr., Phys. Rev. A 5, 1298 (1972).
[14]E. Ott and W. M. Manheimer, IEEE Trans. Plasma Sci. PS-3, 1 (1975).
[15]P. Sprangle and W. M. Manheimer, Phys. Fluids 18, 224 (1975).
[16]P. Sprangle and A. T. Drobot, IEEE Trans. Microwave Theory Tech. MTT-25, 528 (1977).
[17]K. R. Chu, Phys. Fluids 21, 2354 (1978).
[18]P. Sprangle and R. A. Smith, J. Appl. Phys. 51, 3001 (1980).
[19]K. R. Chu, M. E. Read, and A. K. Ganguly, IEEE

Trans. Microwave Theory Tech. MTT-28, 318 (1980).
[20]L. R. Elias, W. M. Fairbank, J. M. J. Madey, H. A. Schwettman, and T. I. Smith, Phys. Rev. Lett. 36, 717 (1976).
[21]D. B. McDermott, T. C. Marshall, S. P. Schlesinger, R. K. Parker, and V. L. Granatstein, Phys. Rev. Lett. 41, 1368 (1978).
[22]J. L. Hirshfield and J. M. Wachtel, Phys. Rev. Lett. 12, 533 (1964).
[23]A. A. Andronov, V. A. Flyagin, A. V. Gaponov, A. L. Goldenberg, M. I. Petelin, V. G. Usov, and V. K. Yulpatov, Infrared Phys. 18, 385 (1978).
[24]J. L. Seftor, V. L. Granatstein, K. R. Chu, P. Sprangle, and M. E. Read, IEEE J. Quantum Electronics, QE-15, 848 (1979).
[25]M. E. Read, R. M. Gilgenbach, R. Lucey, Jr., K. R. Chu, A. T. Drobot, and V. L. Granatstein, IEEE Trans. Microwave Theory Tech. MTT-28, 875 (1980).
[26]P. W. Smith, IEEE J. Quantum Electron. QE-1, 343 (1965).
[27]G. N. Rapoport, A. K. Nemak, and V. A. Zhurakhovskiy, Radiotekh. Elektron. 12, 633 (1967) [Radio Eng. Electron. Phys. (U.S.S.R.) 12, 587 (1967)].
[28]The introduction of a rectangular beam relaxes the perveance requirements by approximately r_0/y_R.